Digitally encoded DNA nanostructures for multiplexed, single-molecule protein sensing with nanopores

Nicholas A. W. Bell and Ulrich F. Keyser**

Cavendish Laboratory, University of Cambridge, JJ Thomson Ave, Cambridge, CB3 0HE, United Kingdom

Corresponding Authors

*E-mail: nawb2@cam.ac.uk, ufk20@cam.ac.uk

Abstract

The simultaneous detection of a large number of different analytes is a continuing challenge for bionanotechnology. Nanopore sensing is an attractive method in this context since it can be integrated into a small and portable device architecture. In this paper, we introduce a technique for multiplexed sensing of single molecules using solid-state nanopores. Based on the principles of DNA origami, we designed a library of DNA nanostructures with each member containing a unique barcode. Each bit in the barcode is signalled by the presence or absence of multiple DNA dumbbell hairpins. We demonstrate 94% accuracy in assignment of a 3-bit barcode by electrophoretically driving the DNA structures through a solid-state nanopore. Selected members of the library are functionalised for detecting a single, specific antibody by antigen presentation at designed positions on the DNA. This allows us to simultaneously detect four different antibodies of the same isotype at nanomolar concentration levels. Our results show the potential of multiple analyte screening using a single-molecule method with binding specificity.

Solid-state nanopores are single-molecule sensors capable of rapidly acquiring significant statistics on a sample in solution and in a label-free manner. The basic method of detection is to analyse modulations in ionic current as molecules pass through a nanopore under an applied potential. This provides information on various aspects of the molecule such as its charge, molecular weight and conformation[1]. The single-molecule nature of the measurement means that it is in principle possible to determine characteristics of individual sub-populations within a complex mixture which could therefore enable the parallel detection of multiple analytes. However inherent limitations, such as the

bandwidth of recording, restrict the resolution available. This means that globular molecules such as proteins show little identifiable differences in their translocation properties when passed through silicon based nanopores[2–4]. A mechanism which imparts chemical selectivity to a nanopore measurement is therefore a crucial step in realising the goal of a highly multiplexed solid-state nanopore sensing platform.

Selectivity for nanopores can be achieved by so-called stochastic sensing which measures the binding on and off of an analyte to a receptor ligand attached to the nanopore surface[5–10] . However stochastic nanopore sensors do not readily lead to the possibility of multi-analyte screening since the attached ligand will be targeted to one or a few similar analytes. Another method that has been explored for imparting selectivity is to use DNA molecules that have binding sites for an analyte of interest and to infer the presence of analytes from the way they modify the interaction of the DNA with a nanopore[11–13]. For solid-state nanopores specific, individual proteins can be detected by engineering programmed binding sites at the centre of a long DNA double-strand[14]. The DNA acts as "carrier" since it then selectively drives proteins through the nanopore.

Here, we build on the idea of the DNA carrier approach, and show the use of DNA nanotechnology to create a powerful combinatorial multiplexing system for solid-state nanopore sensing. Barcode regions are constructed along a long DNA double-strand by using dumbbell hairpin motifs as individual digital bits. We characterize the minimum number of dumbbell hairpins needed for high signal to noise detection and determine the threading dynamics of the barcode signal. We then demonstrate signals from a 3-bit library, yielding eight coded designs, and show an average assignment accuracy of 94%. Selectivity is introduced by tagging members of the library with oligonucleotides which have conjugated binding sites for specific analytes. We demonstrate the potential of this system by simultaneously detecting four different IgG antibodies using a barcoded DNA library and a solitary nanopore.

Barcode design and threading dynamics

Initially we examined how we could create a single digital bit which could be reliably read using a solid-state nanopore. We designed DNA structures with a backbone of double-stranded (ds)DNA and a zone of protruding DNA at the centre (Fig. 1a). The dsDNA backbone is 7228 basepairs (bp) in length and composed of a 7228 base, linear single-strand hybridized to 38 base synthetic oligonucleotides. We chose a so-called DNA dumbbell hairpin as the basic unit of the protruding segment, a motif which was shown as an efficient method for patterning 2D DNA origami[15]. Each dumbbell hairpin has 24 bases which project from the dsDNA backbone and 20 bases which attach it to the backbone. The dumbbell hairpins are spaced at 20 bp intervals therefore forming a left-handed helix around the dsDNA backbone with a twist of 34.3° per unit and inter-unit spacing of 6.8 nm (assuming 10.5 bp/turn dsDNA and 0.34 nm/bp dsDNA separation – Fig. 1b). DNA structures with 5, 11, 17, 23 and 29 dumbbell hairpins at the centre were designed and tested in order to determine the minimum number needed to form a signal that could be readily detected against the background noise. Each design was assembled by mixing the "scaffold" 7228 base strand together with the appropriate DNA oligonucleotide set and annealing in a one-pot reaction for 50 minutes. For all translocation measurements in this paper, we used conical quartz nanopores (Fig. 1c) which gave levels of 105-170 pA for the current blockade level of the backbone dsDNA which is consistent with diameters of 14±3 nm (mean±s.d.) estimated from scanning electron microscopy (Supplementary Section 1). A sorting algorithm (Supplementary Section 2) was written to select events where the DNA passed unfolded through the nanopore (therefore rejecting events with folds or knots[16]) and remove fragments of DNA from the analysis[14].

Representative translocation events with N=5, N=17 and N=29 dumbbell hairpins show a consistent signal at the centre of each translocation due to the passage of the dumbbell hairpins (Fig. 1d). The width and amplitude of the signal increase with the number of dumbbell hairpins since the conical

nanopores used have an effective sensing length on the order of 200 nm[17]. The RMS noise of these nanopores, in the 50 kHz bandwidth used, is 6 pA at 0 mV. On application of 600 mV potential (used for all experiments) this rises due to the variable 1/f noise present in solid-state nanopores[18,19] and we only used nanopores with ~6-12 pA RMS noise at 600 mV (Supplementary Section 2). The number of hairpins used to form a single bit in a barcode is then a compromise between fewer dumbbell hairpins which allows more bits to be placed on the DNA strand and more hairpins which gives a stronger signal for each bit allowing higher read accuracy (Fig. 1e). From these considerations we chose 11 dumbbells as the basic unit forming one digital bit.

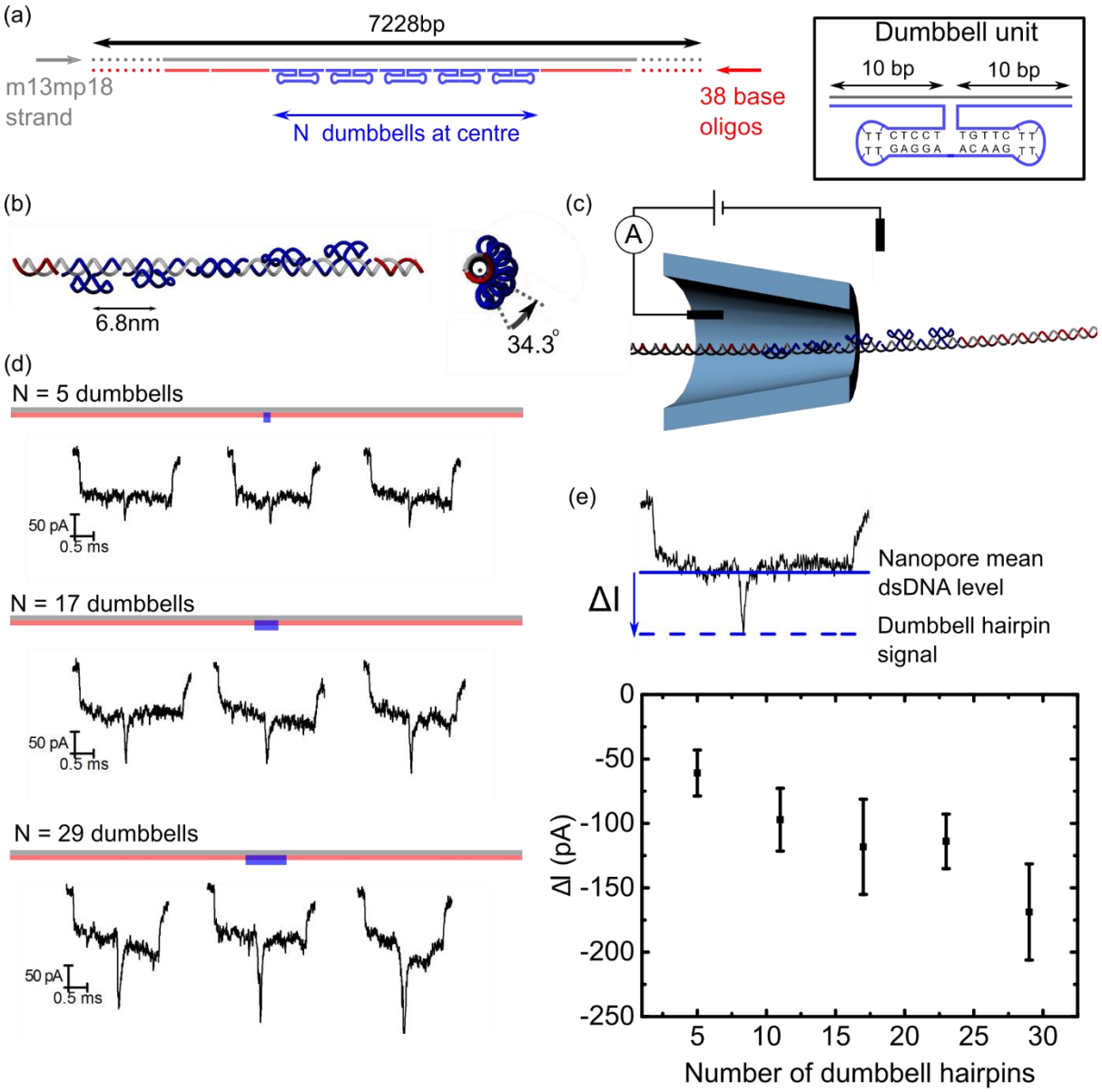

Figure 1 Signal for a single bit formed from dumbbell hairpins. (a) 2D Schematic of DNA structure which is 7228 bp in length and primarily made of 38 base oligonucleotides (red) complementary to the scaffold strand (grey). In the centre, a varying number of oligonucleotides with dumbbell hairpin motifs (blue) are positioned. Inset: Base sequence of dumbbell hairpin motif which is joined onto the backbone by two 10 bp sections. (b) 3D rendering of central dumbbell hairpin section with N=5 dumbbell hairpins. The dumbbell hairpins form a left-handed helix with 34.3° twist between units. (c) Schematic of translocation of 5 dumbbell hairpin design through a conical quartz nanopore. In all experiments 600 mV applied potential was used. (d) Typical translocations with N=

5, 17 and 29 dumbbell hairpins. (e) Statistics on the current change as a function of the number of dumbbell hairpins in the centre. Each sample was measured with a separate nanopore but with similar mean dsDNA levels of 109 pA (N=5 dumbbells), 121 pA (N=11 dumbbells), 111 pA (N=17 dumbbells), 106 pA (N=23 dumbbells) and 113 pA (N=29 dumbbells). Each data point shows the mean±s.d. from a Gaussian fit to all translocations measured.

Having determined the signal size needed for an accurate readout, we designed a DNA structure with five sections each consisting of 11 consecutive dumbbell hairpins (Fig. 2a). Each section of dumbbell hairpins occupies 220 bp on the DNA backbone. The sections are separated by 312 bp which allows for each one to be separately resolved during the translocation. The first section begins 954 bp along the dsDNA backbone. This gives sufficient distance to differentiate the first section from a translocation where the DNA passes through with a single fold at the beginning of the translocation which is the predominant non-single file threading mode[20].

We then calculated a velocity profile of the DNA structure - a pre-requisite for accurate barcode identification. The DNA structure can translocate through a nanopore in one of two polarities with the barcode being at the beginning or end of the translocation. For translocations identified as showing five peaks, we separated these two populations and calculated the translocation time of the 2nd, 3rd, 4th and 5th peaks with respect to the 1st peak (Fig. 2b). In general, the translocation of a polymer through a nanopore is a stochastic drift-diffusion process with the drift due to the applied electric field[21]. We observe that the average translocation velocity is constant in the portion of the DNA structure where the peaks occur (Fig. 2b and Supplementary Section S3). The increase in spread in translocation times of successive peaks reflects the fluctuations in the velocity of the DNA and restricts the accuracy in knowledge of the read position. The source of these fluctuations is larger than that expected from diffusional Brownian motion[22] and may be partly explained by variations in the initial DNA conformation when it is captured by the nanopore[23].

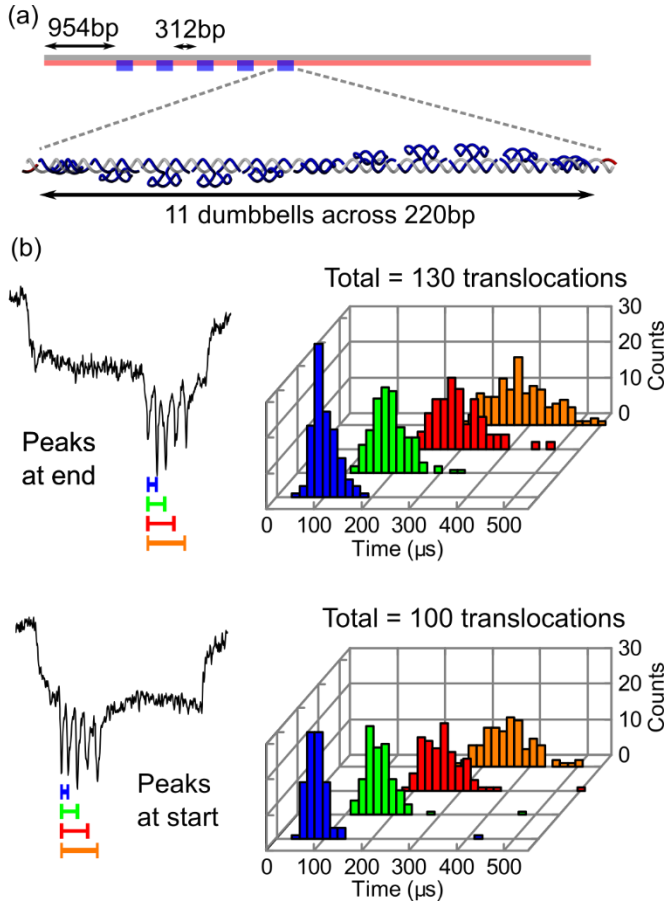

Figure 2 Design and nanopore measurement of DNA structure with multiple zones of protruding secondary structure. (a) Schematic of DNA structure with five protruding sections, each section containing 11 dumbbell hairpins. (b) Translocations showing the barcode occurring at the beginning and end of the translocation (all 230 translocations were measured using the same nanopore). The graphs show histograms of the translocation times of successive peaks relative to the first peak.

Barcode library design

Based on the observed spread in peak translocation times, we designed the following strategy for creating a library of barcodes which could be identified accurately. The first and fifth zones of dumbbell hairpins were always maintained and act as two time markers for signalling the beginning and end of barcode reading (Fig. 3a). The three dumbbell hairpin zones between these two can each be assigned a "1" value by keeping the dumbbell hairpins or a "0" value by replacing the dumbbell hairpins with oligonucleotides which simply form a double-strand with the scaffold. Therefore by mixing the appropriate oligonucleotide sets we synthesised a library of 2^3=8 different barcodes. These eight designs were each separately translocated through a nanopore (Fig. 3). A baseline correction and peak detection algorithm was used to locate the position of each peak in the translocation signal (Supplementary Section S2) and assign a barcode that best matched the peak locations based on a constant velocity expectation between the first and last peaks (Fig. 3b). Typical translocations clearly show the barcodes corresponding to the expected design (Fig. 3c). For measurements where a single library member was added to the sample reservoir, the average correct assignment of a barcode is 94±3% (mean±s.d.) taken across N=25 nanopore measurements of the eight library members (Fig.3c and Supplementary Section S4).

We also investigated the percentage of correctly assigned barcodes when four members of the library were mixed together at equimolar concentration. For two separate mixtures containing only four codes we observe high assignment percentages for the four barcodes present (Fig. 3d). 97±1% (mean±s.d.) of assigned barcodes are one of the four designs in the mixture (Supplementary Section S4). Furthermore when the entire library is mixed in an equimolar ratio we observe an approximately equal assignment of barcodes again indicating the high read accuracy in the system.

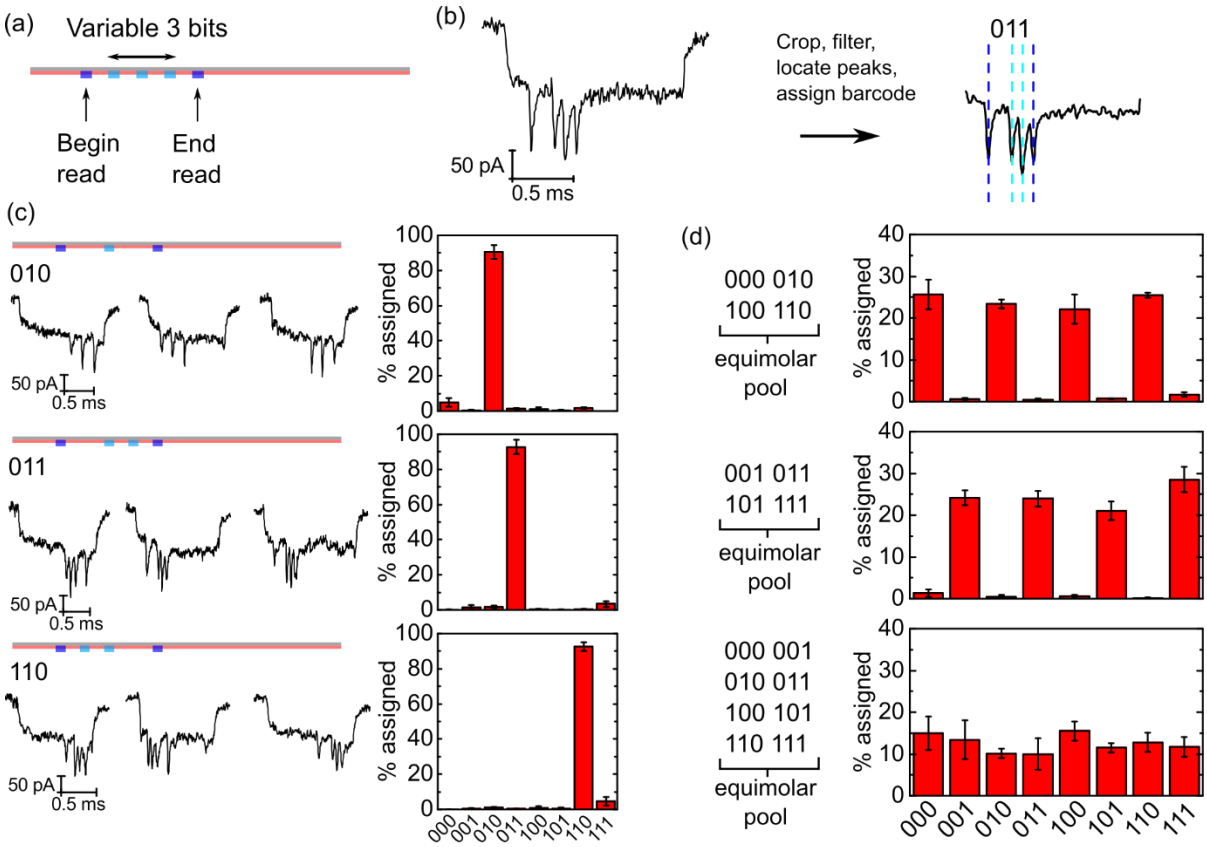

Figure 3 Multiplexed barcode design and readout efficiency. (a) The first and last zones on the DNA nanostructure signify start read and end read instructions and the middle three zones are bits which can be assigned "0" or "1" with different oligonucleotides mixes. (b) Workflow of barcode assignment algorithm – each translocation is cropped and filtered before the peaks are located. The first and last peaks are used as time markers and the barcode is assigned based on the closest match of the variable peaks to the expected time positions. (c) Example translocations of three library members and their barcode assignment efficiency (histograms show mean±s.d.) averaged over separate nanopores. 010 (N=3 nanopores, 456 translocations total), 011 (N=4 nanopores, 613 translocations total), 110 (N=5 nanopores, 1465 translocations total). (d) Barcode assignment percentages of equimolar mixtures containing indicated library members. The mixtures were 000, 010, 100, 110 (N=3 nanopores, 1578 translocations total); 001, 011, 101, 111 (N=5 nanopores, 1211 translocations total); and a mixture of all 8 barcodes (N=5 nanopores, 1095 translocations total).

Binding site presentation

Having successfully developed a barcode strategy, we tested the ability of one member of the library to selectively detect an IgG isotype antibody. We took the oligonucleotide set for the 011 barcode and designed a binding site for an antibody to the synthetic nucleoside bromodeoxyuridine (BrdU). IgG antibodies have two identical binding sites on each arm and can bind epitopes with a spacing of approximately 6-12 nm[24,25]. The multivalent binding of both arms can significantly increase the overall dissociation constant compared to binding of a single arm[26]. We therefore developed the following strategy to take advantage of the ability to engineer the position of the binding sites on the DNA for high antibody affinity. A 31 base oligonculeotide was positioned ¾ of the way along the contour of the DNA structure. The 5' end was modified with a short spacer of 8 thymine nucleotides conjugated to the BrdU antigen. The 5' end of the next oligonucleotide along the backbone was also modified with 8 thymines and BrdU. The spacing of the two 8 thymine + BrdU motifs is therefore 31 bp (10.5 nm) along the duplex – approximately three full rotations around the double helix – so that the antibody binds via a divalent attachment. 10.5 nm is significantly smaller than the persistence

length of dsDNA (~50 nm) so the DNA backbone behaves effectively as a rigid rod on this scale. Consequently, the binding of both antibody arms should not cause a significant free energy penalty for the DNA backbone which helps to increase the binding affinity[26]. The 8 thymine spacer gives some distance between the DNA backbone and antibody to prevent steric repulsion while also giving flexibility to the antigen positions so that they are easily accessible to the two arms of the antibody.

The DNA structure was incubated with a ten-fold stoichiometric excess of antibody before being transferred into the buffer used for nanopore measurements with a final concentration of 4 nM of DNA structures and 40 nM antibody in the sample reservoir. This results in several DNA structure translocations per second[17]. The ionic current signatures of the DNA structure translocation are easily separated from those of the free antibody based on the total charge excluded during the translocation, as demonstrated before[14] (Supplementary Section S2). The DNA structure translocation events showed a characteristic peak at ¾ of the contour length indicating the presence of the bound antibody. Each translocation was analysed by splitting the translocation into two equal sections, assigning a barcode to one section and performing a threshold peak search in the other section to determine the presence or absence of the antibody (Fig. 4b). We specifically designed the barcode section to occur within one half of the translocation so that this simple method of separating the two sections could be performed.

The 011 barcode assignment percentage of the BrdU modified DNA structure is similar for translocations after incubation with the antibody (91±4%, mean±s.d., N=3 pores) compared to controls where the antibody was not added (95±3%, mean±s.d., N=7 pores). This indicates that the presence of the antibody does not significantly affect the dynamics of the DNA. Indeed we observe a narrow distribution in the transit times of the antibody (Supplementary Section S5) thereby suggesting an absence of strong surface interactions between the antibody and the diameter of nanopores used here. The narrow distribution may reflect the fact that a large translocation force is imparted onto the antibody through the electrophoretic force acting on the DNA and the strong coupling between the dual antigen binding sites and the antibody.

The percentage of translocations showing a positive peak in the non-barcode half (calculated from only those translocations that are assigned a 011 barcode) shows a substantial difference between the DNA structure incubated with antibody and the control. 97±1% (N=3 pores, mean±s.d,) of 011 translocations showed a positive peak after antibody incubation. In comparison, the control exhibited only 4±2% (N=7 pores, mean±s.d) of translocations with a positive signal. These false positives are likely to be due to complicated folding patterns or knots in the DNA which are not filtered out by the analysis algorithm (Supplementary Section S2). The substantial difference in positive signals after antibody incubation demonstrates that we are able to clearly detect the antibody presence on the barcoded DNA.

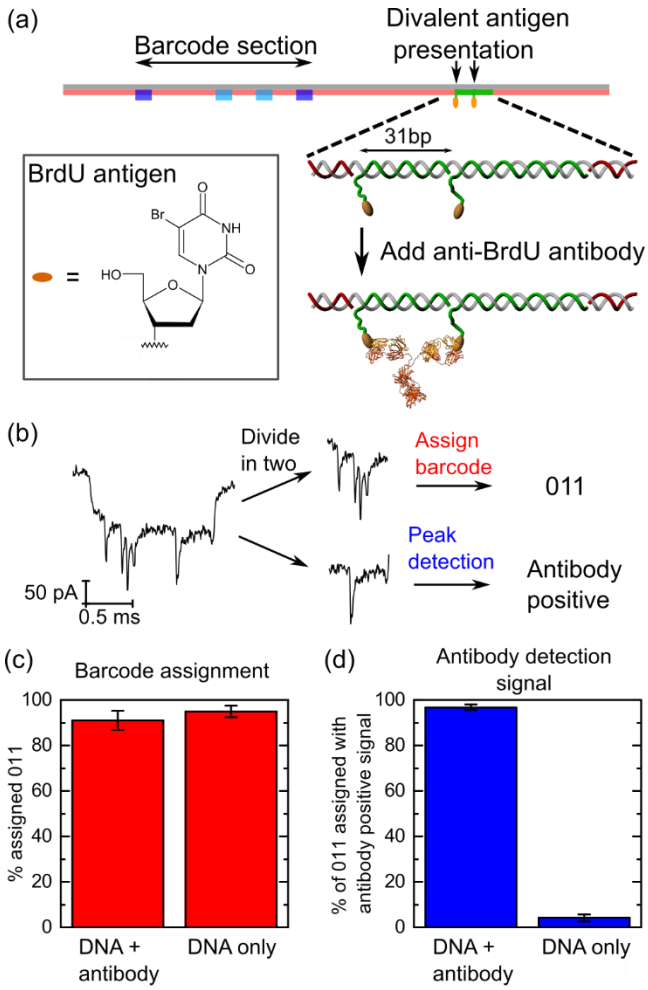

Figure 4 – Binding site presentation and analysis for bound antibody in translocations. (a) Antigen presenting scheme on the DNA nanostructure. Two oligonucleotides (green) at ¾ of the DNA contour length are extended at the 5' end with an 8 thymine overhang conjugated to the antigen. The overhangs are separated by 31 bp = 10.5 nm. The particular example used here is a 011 barcode with BrdU as the antigen. (b) Typical translocation of the DNA after incubation with anti-BrdU antibody. All translocations are analysed by splitting into two halves then determining the barcode from one half and performing a threshold peak search which yields a call of either antibody positive or antibody negative. The particular example shown here registered as antibody positive. (c) Comparison of percentage of 011 assigned translocations when incubated with antibody and for a control without antibody present. Error bars show s.d. from averaging over separate nanopores. (d) Comparison of positive signal percentage for only those translocations assigned a 011 barcode.

Multiplexed sensing

Having established a robust barcoding and antibody binding strategy, we tested the ability to multiplex measurements for simultaneous detection of four antibodies. Four members of the eight member barcode library were modified with two 31 bp spaced tags terminated with small molecule antigens. The barcode and tagged antigen combinations (each also tested separately see Supplementary Section S5) were as follows: 001 = biotin, 011 = BrdU, 101 = puromycin, 111 = digoxigenin (Fig. 5a). The remaining four barcodes 000, 010, 100 and 110 (containing only 8 thymine overhangs with no antigen conjugated) were mixed in an equimolar ratio with the antigen presenting barcodes and act as controls. The equimolar library was then mixed with antibodies to all four antigen labelled designs so that the final concentrations in the nanopore reservoir were 0.5 nM of each DNA barcode and 10 nM of each antibody (Fig. 5b). Gel shift assays indicated no appreciable

cross-reactivity between these antibodies (Supplementary Section S6). The percentage of barcodes assigned from all translocations is approximately equal for all members of the library (Fig. 5c). This result shows that the ~150 kDa antibody does not significantly affect the electrokinetics of the ~5 MDa barcoded DNA nanostructures. The percentage of positive antibody signals correlates with the four antibody targeting barcodes (Fig. 5d). Two proportion tests between the positive antibody signals on the control barcodes and the antigen tagged barcodes showed significantly (p-value<0.001) more positives on the antigen tagged barcodes (Supplementary Section S7). Therefore these results demonstrate that multiple antibodies can be simultaneously detected using our digitally encoded DNA nanostructure library.

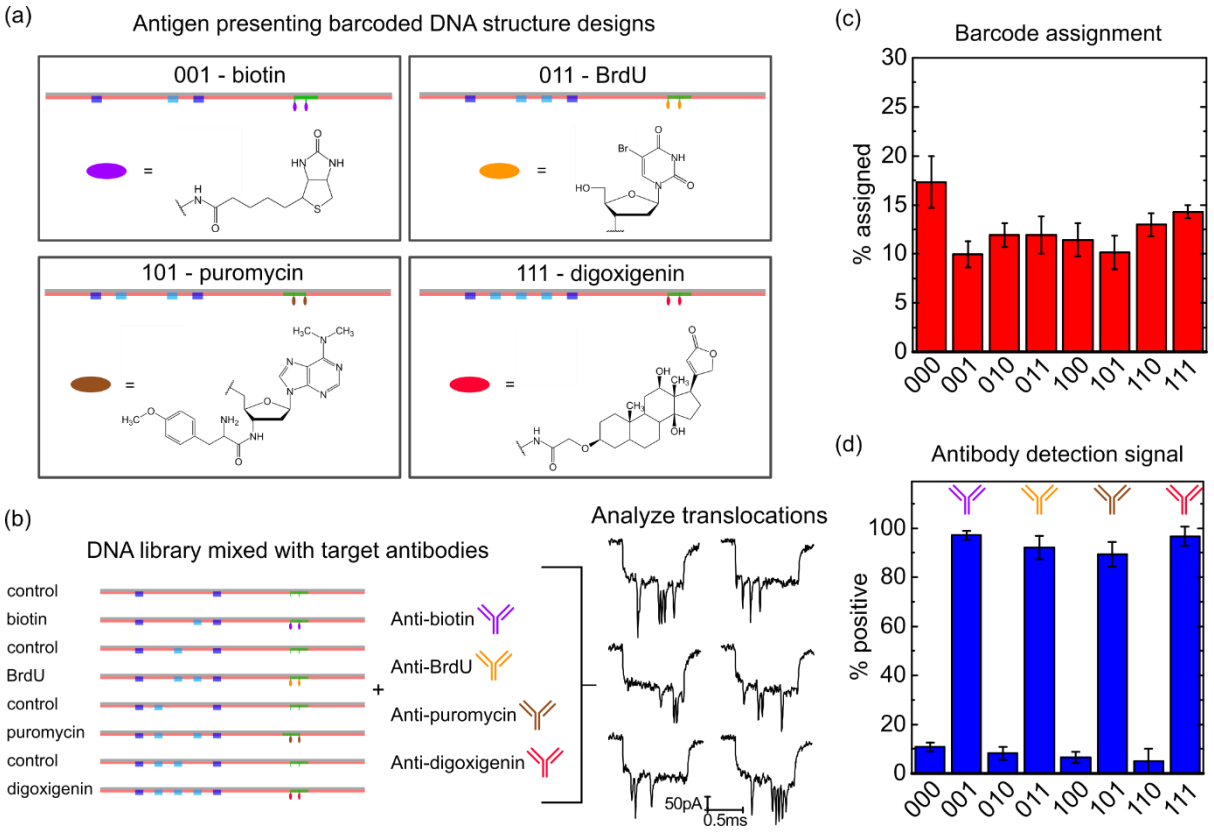

Figure 5 - Selective detection of multiple antibodies. (a) Four members of the library are modified with binding motifs for biotin, BrdU, puromycin and digoxigenin. (b) Each barcoded design was mixed in an equimolar ratio with the other four members of the multiplex library which carried 8 thymine overhangs but no antigen. Antibodies to the four antigen species were then mixed and nanopore translocations analysed. (c) Barcode assignment percentage showing a uniform distribution as expected for the equimolar mix (N=6 nanopores, mean±s.d.). (d) Protein detection signal percentages for the assigned barcodes. The total number of assigned translocations from all nanopores was 5711.

In summary, we have presented a new method for multiplexing solid-state nanopore sensing of proteins by programming barcodes of protruding structure along a DNA double-strand which also contain a high affinity binding site. We used the tools of DNA nanotechnology to engineer these barcodes for efficient detection. Our basic design of a 3-bit code could be significantly expanded for instance by using a longer single-stranded DNA scaffold[27]. Advances in high bandwidth amplifiers and high sensitivity nanopores in thin membranes[28] will also enable greater multiplexing via a reduction in the number of dumbbell hairpins required to signal one bit. In both cases the fluctuations in DNA velocity during translocation need to be accurately characterized, as we have shown here, to

enable high readout accuracy of the barcode. A further improvement is possible by engineering stiffer DNA structures which would reduce the number of false positives due to folded DNA configurations. For example six helix bundles have an approximately 20 fold higher persistence length than double-stranded DNA[29,30] and nanopore translocations on similarly high persistence length filamentous fd virus indicate that such structures stiff structures translocate without folding[31].

We anticipate that a range of DNA conjugation techniques could be used to engineer binding sites onto the structure. For instance recombinant tags are widely used for DNA attachment with high yield[32,33]. The technique is generalizable to any analyte sensing as long as the selective binding site can be conjugated onto a DNA oligonucleotide. However, a significant molecular weight contrast between the binding site and its target analyte will be necessary in future designs so that the ionic current reduction is identifiably different with and without the bound analyte. A "sandwich" assay approach of adding an antibody which binds to the DNA-analyte complex could potentially be used to improve the molecular weight contrast – analogous to the reduction in gel mobility using a supershift electrophoretic mobility assay. It should also be possible to determine the concentration of analytes by measuring changes in the number of positive signals, indicating bound analyte, as a function of analyte and DNA concentrations. Further efforts to reduce the false positive detection rate will help in this regard to increase the achievable dynamic range. The continuing development of DNA conjugation methods will also enable further possibilities for simple addition of binding sites onto the structure. These advances combined with arrays of multiple nanopores should enable a rapid and specific method for assaying multiple analytes with potential applications in research and diagnostics.

Methods

Nanopore fabrication and measurement

Nanopores were fabricated by laser-assisted pulling (Sutter P-2000) of quartz glass capillaries with inner diameter 0.2 mm. Each nanopore was then integrated into a polydimethylsiloxane (PDMS) device[34]. A total of 47 different nanopores were used in this paper (Supplementary Section S8). The device was filled with a measurement buffer of 10 mM Tris-HCl (pH 8), 1 mM $MgCl_2$, 50 mM NaCl, 4 M LiCl. Ionic currents were recorded using a resistive feedback amplifier (Axopatch 200B, Molecular Devices) with an external 8-pole low pass Bessel filter (Frequency Devices) set to 50 kHz and sampled at 250 kHz using a 16-bit data acquisition card (National Instruments). All analytes were added to the reservoir containing the nanopore tip which was set as the electrical ground and a potential of +600 mV was applied in all experiments.

Synthesis of DNA nanostructures

M13mp18 ssDNA was purchased from New England Biolabs. Approximately 90% is in a circular form and the DNA was linearised by hybridizing with a 39 base oligonucleotide and cutting at the BamHI and EcoRI sites. The linearised scaffold was then mixed with the appropriate oligonucleotide set at a 1:5 stoichiometric ratio of scaffold:oligonucleotide and annealed for 50 minutes (Supplementary Section S10). Excess oligonucleotides were removed by ultrafiltration with Amicon Ultra filters. In all experiments the final concentration of DNA nanostructures in the nanopore reservoir was 4 nM (therefore 4 nM when analysing an individual design, 1 nM of each design when four designs are mixed together and 0.5 nM of each design when eight designs are mixed together).

Antibody binding

Affinity isolated goat polyclonal anti-biotin (Sigma, B3640), mouse monoclonal anti-BrdU (Abcam ab8039), mouse monoclonal anti-puromycin (Merck, MABE343) and mouse monoclonal anti-digoxigenin (Roche, 11333062910) were purchased. The binding of each antibody to a short duplex of DNA containing two antigens was tested by agarose gel electrophoresis (Supplementary Section S6). For nanopore measurements, each antibody was incubated with its respective barcoded DNA

nanostructure by incubating 8 nM of the barcoded DNA structure with 80 nM antibody in 10 mM Tris-HCl (pH=8), 2 mM $MgCl_2$, 100 mM NaCl for 30 minutes at room temperature. For individual measurements (Supplementary Section S5), this mixture was then flushed into the nanopore sample reservoir so that the final concentration was 4 nM DNA and 40 nM antibody in 10 mM Tris-HCl (pH=8), 1 mM $MgCl_2$, 50 mM NaCl, 4M LiCl. For the multiplexed measurements of Figure 5, a mixture containing 8 nM DNA (1 nM of each of the eight designs) and 80 nM antibody (containing 20 nM of each of the four antibodies) was incubated for 30 minutes before adding for nanopore measurements so that the final concentration of DNA was 0.5 nM of each design together with 10 nM of each antibody. Analysis of the number of positive signals showed no observable unbinding over the timecourse of a typical nanopore experiment in this electrolyte (Supplementary Section S7).

Open data

Raw data traces for all translocations together with data files on barcode assignments will be available in an online repository.

Acknowledgements

The authors thank J. Kong and V. Thacker for useful discussions. N.A.W.B. acknowledges funding from an EPSRC doctoral prize award, an ERC starting grant (Passmembrane 261101) and an ERC consolidator grant (Designerpores 647144). U.F.K. acknowledges support from an ERC starting grant (Passmembrane 261101) and an ERC consolidator grant (Designerpores 647144).

1. Wanunu, M. Nanopores: A journey towards DNA sequencing. *Phys. Life Rev.* **9,** 125–58 (2012).

2. Li, W. *et al.* Single protein molecule detection by glass nanopores. *ACS Nano* **7,** 4129–4134 (2013).

3. Plesa, C. *et al.* Fast translocation of proteins through solid state nanopores. *Nano Lett.* **13,** 658–663 (2013).

4. Firnkes, M., Pedone, D., Knezevic, J., Döblinger, M. & Rant, U. Electrically Facilitated Translocations of Proteins through Silicon Nitride Nanopores: Conjoint and Competitive Action of Diffusion, Electrophoresis, and Electroosmosis. *Nano Lett.* **10,** 2162–2167 (2010).

5. Bayley, H. & Martin, C. R. Resistive-pulse sensing from microbes to molecules. *Chem. Rev.* **100,** 2575–2594 (2000).

6. Bayley, H. & Cremer, P. S. Stochastic sensors inspired by biology. *Nature* **413,** 226–30 (2001).

7. Braha, O. *et al.* Designed protein pores as components for biosensors. *Chem. Biol.* **4,** 497–505 (1997).

8. Rotem, D., Jayasinghe, L., Salichou, M. & Bayley, H. Protein detection by nanopores equipped with aptamers. *J. Am. Chem. Soc.* **134,** 2781–2787 (2012).

9. Movileanu, L., Howorka, S., Braha, O. & Bayley, H. Detecting protein analytes that modulate transmembrane movement of a polymer chain within a single protein pore. *Nat. Biotechnol.* **18,** 1091–1095 (2000).

10. Wei, R., Gatterdam, V., Wieneke, R., Tampé, R. & Rant, U. Stochastic sensing of proteins with receptor-modified solid-state nanopores. *Nat. Nanotechnol.* **7,** 257–263 (2012).

11. Li, T., Liu, L., Li, Y., Xie, J. & Wu, H.-C. A Universal Strategy for Aptamer-Based Nanopore Sensing through Host-Guest Interactions inside α-Hemolysin. *Angew. Chemie* **127,** 7678–7681 (2015).

12. Kawano, R. *et al.* Rapid detection of a cocaine-binding aptamer using biological nanopores on a chip. *J. Am. Chem. Soc.* **133,** 8474–8477 (2011).

13. Kasianowicz, J. J., Henrickson, S. E., Weetall, H. H. & Robertson, B. Simultaneous multianalyte detection with a nanometer-scale pore. *Anal. Chem.* **73,** 2268–2272 (2001).

14. Bell, N. A. W. & Keyser, U. F. Specific Protein Detection Using Designed DNA Carriers and Nanopores. *J. Am. Chem. Soc.* **137,** 2035–2041 (2015).

15. Rothemund, P. W. K. Folding DNA to create nanoscale shapes and patterns. *Nature* **440,** 297–302 (2006).

16. Steinbock, L. J., Otto, O., Chimerel, C., Gornall, J. & Keyser, U. F. Detecting DNA folding with nanocapillaries. *Nano Lett.* **10,** 2493–2497 (2010).

17. Bell, N. A. W., Muthukumar, M. & Keyser, U. F. Translocation frequency of double-stranded DNA through a solid-state nanopore. *Phys. Rev. E* ***93****, 022401* (2016).

18. Smeets, R. M. M., Keyser, U. F., Dekker, N. H. & Dekker, C. Noise in solid-state nanopores. *Proc. Natl. Acad. Sci.* **105,** 417–21 (2008).

19. Tabard-Cossa, V., Trivedi, D., Wiggin, M., Jetha, N. N. & Marziali, A. Noise analysis and reduction in solid-state nanopores. *Nanotechnology* **18,** 305505 (2007).

20. Storm, A., Chen, J., Zandbergen, H. & Dekker, C. Translocation of double-strand DNA through a silicon oxide nanopore. *Phys. Rev. E* **71,** 1–10 (2005).

21. Muthukumar, M. Mechanism of DNA transport through pores. *Annu. Rev. Biophys. Biomol. Struct.* **36,** 435–50 (2007).

22. Chen, P. *et al.* Probing Single DNA Molecule Transport Using Fabricated Nanopores. *Nano Lett.* **4,** 2293–2298 (2004).

23. Lu, B., Albertorio, F., Hoogerheide, D. P. & Golovchenko, J. A. Origins and consequences of velocity fluctuations during DNA passage through a nanopore. *Biophys. J.* **101,** 70–79 (2011).

24. Saphire, E. O. *et al.* Contrasting IgG structures reveal extreme asymmetry and flexibility. *J. Mol. Biol.* **319,** 9–18 (2002).

25. Preiner, J. *et al.* IgGs are made for walking on bacterial and viral surfaces. *Nat. Commun.* **5,** 1–8 (2014).

26. Mammen, M., Choi, S.-K. & Whitesides, G. M. Polyvalent Interactions in Biological Systems: Implications for Design and Use of Multivalent Ligands and Inhibitors. *Angew. Chemie Int. Ed.* **37,** 2754–2794 (1998).

27. Marchi, A. N., Saaem, I., Vogen, B. N., Brown, S. & LaBean, T. H. Towards larger DNA origami. *Nano Lett* **14,** 5740–5747 (2014).

28. Rosenstein, J. K., Wanunu, M., Merchant, C. A., Drndic, M. & Shepard, K. L. Integrated nanopore sensing platform with sub-microsecond temporal resolution. *Nat. Methods* **9,** 487–492 (2012).

29. Kauert, D. J., Kurth, T., Liedl, T. & Seidel, R. Direct mechanical measurements reveal the material properties of 3D DNA-origami. *Nano Lett.* **11,** 5558–63 (2011).

30. Castro, C. E., Su, H.-J., Marras, A. E., Zhou, L. & Johnson, J. Mechanical design of DNA nanostructures. *Nanoscale* **7,** 5913–5921 (2015).

31. McMullen, A., de Haan, H. W., Tang, J. X. & Stein, D. Stiff filamentous virus translocations through solid-state nanopores. *Nat. Commun.* **5,** 4171 (2014).

32. Fu, J., Liu, M., Liu, Y. & Yan, H. Spatially-Interactive Biomolecular Networks Organized by Nucleic Acid Nanostructures. *Acc. Chem. Res.* **45,** 1215–1226 (2012).

33. Pippig, D. A., Baumann, F., Strackharn, M., Aschenbrenner, D. & Gaub, H. E. Protein-DNA chimeras for nano assembly. *ACS Nano* **8,** 6551–6555 (2014).

34. Bell, N. A. W. *et al.* Multiplexed ionic current sensing with glass nanopores. *Lab Chip* **13,** 1859–62 (2013).